Noname manuscript No.
(will be inserted by the editor)

Simulations of Light Antinucleus–Nucleus Interactions

A. Galoyan · V. Uzhinsky

Received: date / Accepted: date

Abstract Creations of light anti-nuclei (anti-deuterium, anti-tritium, anti-^{3}He and anti-^{4}He) are observed by collaborations at the LHC and RHIC accelerators. Some cosmic ray experiments are aimed to find the anti-nuclei in cosmic rays. To support the experimental studies of anti-nuclei a Monte Carlo simulation of anti-nuclei interactions with matter is implemented in the GEANT4 toolkit. The implementation combines practically all known theoretical approaches to the problem of antinucleon-nucleon interactions.

Keywords anti-nucleus · anti-proton · cross sections · annihilation · quark-gluon string model

PACS 25.43.+t · 13.75.Cs · 21.60.Ka · 25.45.-z · 25.45.De

1 Introduction

One of the most exciting puzzles in cosmology is connected with the question of the existence of anti-matter in the Universe. A number of dedicated cosmic ray experiments aim to search for anti-nuclei [1–4]. Also, anti-nuclei have been observed in nucleus-nucleus and proton-proton collisions by experiments at the RHIC [5–7] and LHC accelerators [8]. The STAR collaboration at RHIC reported in March 2011 that the anti-^{4}He nuclei were identified in high energy nucleus-nucleus collisions (see [9]). The ALICE collaboration at LHC confirmed the STAR results in May 2011.

On behalf of the Geant4 Hadronics Working Group

A. Galoyan
LHEP, JINR, Dubna, Russia
Tel.: +7496-21-64049
E-mail: galoyan@lxmx00.jinr.ru

V. Uzhinsky
LIT, JINR, Dubna, Russia and CERN, Geneva, Switzerland

An experimental study of anti-nuclei requires a knowledge of anti-nucleus interaction cross sections with matter. The cross sections are needed to estimate various experimental corrections, especially those due to particle losses which reduce the detected rate. In practice, various phenomenological approaches are applied in order to estimate the antinucleus-nucleus cross sections. Thus, the first task is a creation of reliable estimations of the cross sections. Here we use the Glauber approach.

It is obvious that an annihilation can take place at an interaction of an anti-nucleus with a nucleus. A lot of mesons can be produced in this way. Thus, we have to simulate the meson production. We do this in the framework of the quark-gluon string model.

Low energy mesons can have secondary interactions in nuclear residues. We take them into account using the binary cascade model of the GEANT4 toolkit [10].

2 Antinucleus-nucleus cross sections

Anti-proton elastic scattering by deuterons was considered in the classic paper by V. Franco and R.J. Glauber [11]. O.D. Dalkarov and V.A. Karmanov [12] showed that elastic and inelastic (with excitation of nuclear levels) anti-proton scattering by C, Ca, and Pb nuclei are described quite well at $\bar{p}$ kinetic energies of 46.8 and 179.7 MeV. The first calculations of the cross sections of anti-deuteron interactions with nuclei in the eikonal approximation were presented by Buck et al. [13] (see also [14]). Cross sections of antideuteron-deuteron interactions at an antideuteron momentum of $P_{\bar{d}} = 12.2$ GeV/c were calculated using the Glauber approach in [15]. They were in good agreement with the experimental data. We use the Glauber approach to calculate the antinucleus-nucleus cross sections.

The elastic scattering amplitude of an anti-nucleus containing $\bar{A}$ anti-baryons on a target nucleus with mass number A is given as [16]:

$$F_{\bar{A}A}(\mathbf{q}) = \frac{i}{2\pi} \int d^2b\ e^{i\mathbf{qb}} \left\{ 1 - \prod_{i=1}^{\bar{A}} \prod_{j=1}^{A} [1 - \gamma(\mathbf{b} + \boldsymbol{\tau}_i - \mathbf{s}_j)] \right\} |\Psi_{\bar{A}}|^2 |\Psi_A|^2 \cdot \left(\prod_{i=1}^{\bar{A}} d^3\ t_i \right) \left(\prod_{j=1}^{A} d^3\ r_j \right) = i \int_0^\infty b P_{\bar{A}A}(b)\ J_0(qb) db, \tag{1}$$

where the same nomenclature is used as described in [16,12] .

The main ingredients of the approach are parameterizations of energy dependencies of total and elastic antinucleon-nucleon scatterings. We have considered the parameterizations in our recent publication [17]. Using them, one can calculate various cross sections of antiproton-nucleus and antinucleus-nucleus interactions.

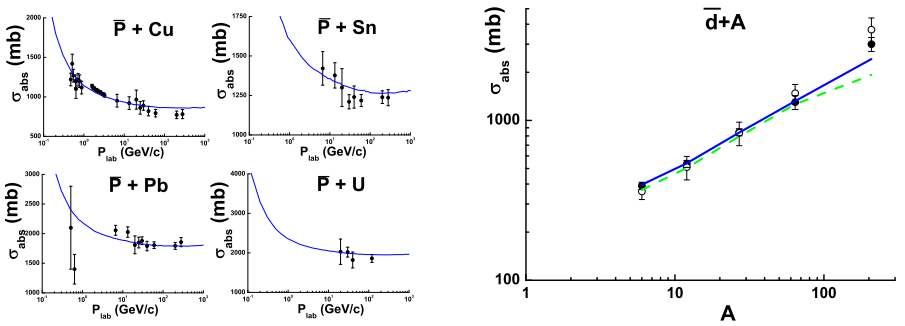

Fig. 1 Absorption cross sections of anti-proton and anti-deuteron interactions with nuclei. Left figure, the points are experimental data from the Durham data base, the lines are our calculations. Right figure, the solid and open points are the experimental data [18] at anti-deuteron momenta of 13.3 and 25 GeV/c, the solid and dashed lines are, correspondingly, our calculation results.

We show in Fig. 1 the results of our calculations in a comparison with experimental data. For projectile anti-deuterons, we present data at two momenta ([18]), 13.3 and 25 GeV/c (open and close circles, correspondingly), and the results of a calculation at the energies (solid and dashed lines). As can be seen, the agreement between the experimental data and the calculations is rather good.

The profile function, $P_{\bar{A}A}(b)$, of the elastic antinucleus-nucleus scattering is very close to the 2-dimensional Fermi-function, $P_{\bar{A}A}(b) = 1/[1 + exp((b - R)/c)]$. The Fourier-Bessel transform of the function gives the elastic scattering amplitude in the momentum representation. We use analytical expression for an expansion of the transform presented in ([19]) to calculate differential elastic antinucleus-nucleus cross sections.

Calculations of the total, inelastic and elastic cross-sections of of an anti-nucleus interactions with nuclei allow one to determine a point where the anti-nucleus penetrating through a matter will interact.

3 Simulations of multiparticle production in antinucleon-nucleon interactions

The main channel of the antinucleon-nucleon interactions at low energies is the annihilation into 3, 4, or 5 mesons. It is commonly assumed that the reaction is going through the re-arangement of quarks and anti-quarks in the colliding particles, see Fig. 2a. At high energies, the reaction will result in the creation of three quark-gluon strings.

If a quark and an antiquark annihilate (Fig. 2b), a diquark-antidiquark string will be left. Such a string must fragment into a final state containing a baryon and an anti-baryon. A description of the fragmentation of such strings is one of the problems in high energy physics. We have solved it using experimental data on the reactions $\bar{p}p \to \bar{n}n, \bar{\Lambda}\Lambda, \bar{n}n\pi^0$, and so on.

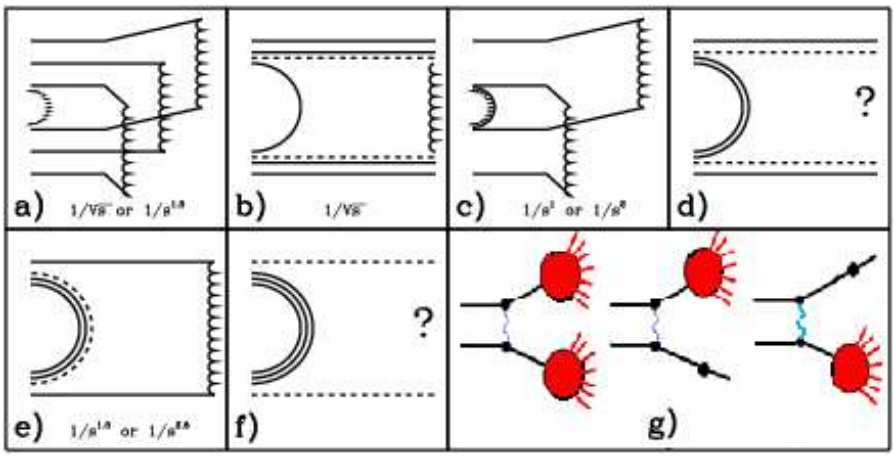

Fig. 2 Quark flow diagram. The solid lines represent quarks, the dashed ones – the string junctions.

A string junction couples quarks in a baryon. The annihilation of the string junctions takes place via the process as illustrated in Fig. 2a which results in a three string creation.

At the annihilation of quark, anti-quark and string junctions, two strings will be created (see Fig. 2c). If the energy is sufficiently low, two mesons will be produced.

The diagrams "d" and "e" describe the processes with one string creation. The ordinary quark-antiquark string can fragment into at least two mesons. A hybrid meson with hidden baryon number can be produced at low energies as depicted in diagram "d" .

It is needed to add the "standard" Fritiof model [20] diagrams "g" at high energies. One or two strings can be created in the corresponding processes without baryon number exchanges.

The main issue of the considered approach is a determination of energy dependencies of the process shown in Fig. 2. We did not find an acceptable theoretical solution of this issue. Thus, we parameterized the cross sections as follow:

$$\sigma_a = \frac{16}{\sqrt{s-4m^2}}\left[(s-4m^2)^{-0.175} + 3.125 * (1 - 1.88/\sqrt{s})\right] \quad \text{(mb)}, \tag{2}$$

$$\sigma_b = 3.13 + 140 \cdot (M_{th} - \sqrt{s})^{2.5} \quad \text{(mb)}, \quad \sqrt{s} \le M_{th} = 2.172 \quad \text{(GeV)}, \tag{3}$$

$$\sigma_b = 6.8/\sqrt{s} \quad \text{(mb)}, \qquad \sqrt{s} > M_{th} = 2.172 \quad \text{(GeV)},$$

$$\sigma_e = 23.3/s \quad \text{(mb)}, \tag{4}$$

$$\sigma_c = \sigma_d = \sigma_f = 0, \tag{5}$$

$$\sigma_g = 35 * (1. - 2.1/\sqrt{s}) \quad \text{(mb)}, \tag{6}$$

where σ_a, σ_b, and so on are cross sections of the processes of Fig. 2, respectively.

The parameterizations of the cross sections and LUND string fragmentation algorithm are implemented in FTF generator of the GEANT4 toolkit [10]. Using this generator, we obtain results presented in Fig. 3. As can be seen, the experimental dependencies are reproduced, though a more refined consideration is needed.

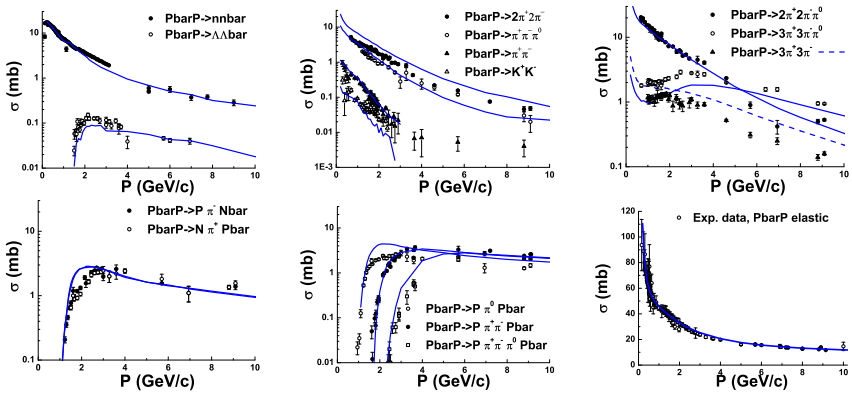

Fig. 3 Reaction cross sections of $\bar{p}p$-interactions. The points are experimental data, the lines are our calculations.

4 Antiproton-nucleus interactions

Cross sections (σ_ν) of various processes in high energy antibaryon-nucleus interactions with different multiplicities (ν) of involved nuclear nucleons can be determined using the elastic scattering amplitude (1) and the asymptotic Abramovsky-Gribov-Kancheli (AGK) cutting rules:

$$\sigma^{in}_{\bar{p}A} = \sum_{\nu=1}^{A} \sigma_\nu, \quad \sigma_\nu = C^\nu_A \int d^2b \left[\frac{1}{A}\int g(\mathbf{b}-\mathbf{s})\rho_A(\mathbf{s},z)d^2s\ dz\right]^\nu \cdot \tag{7}$$

$$\cdot \left[1 - \frac{1}{A}\int g(\mathbf{b}-\mathbf{s})\rho_A(\mathbf{s},z)d^2s\ dz\right]^{A-\nu}, \quad g(\mathbf{b}) = \gamma(\mathbf{b}) + \gamma^*(\mathbf{b}) - \gamma(\mathbf{b})\cdot\gamma^*(\mathbf{b}).$$

At low energies, we have introduced finite energy corrections to the AGK-cutting rules and obtained

$$\sigma^{in}_{\bar{p}A} = \sum_{\nu=1}^{\nu_{max}} \sigma'_\nu, \quad \nu_{max} = [p_{lab}/p_0] + 1, \quad p_0 \simeq 2\ (\mathrm{GeV/c}), \tag{8}$$

$$\sigma'_\nu = C^\nu_{\nu_{max}} \int d^2b \left\{1 - \left[1 - \frac{1}{A}\int g(\mathbf{b}-\mathbf{s})\rho_A(\mathbf{s},z)d^2s\ dz\right]^{A/\nu_{max}}\right\}^\nu \cdot \tag{9}$$

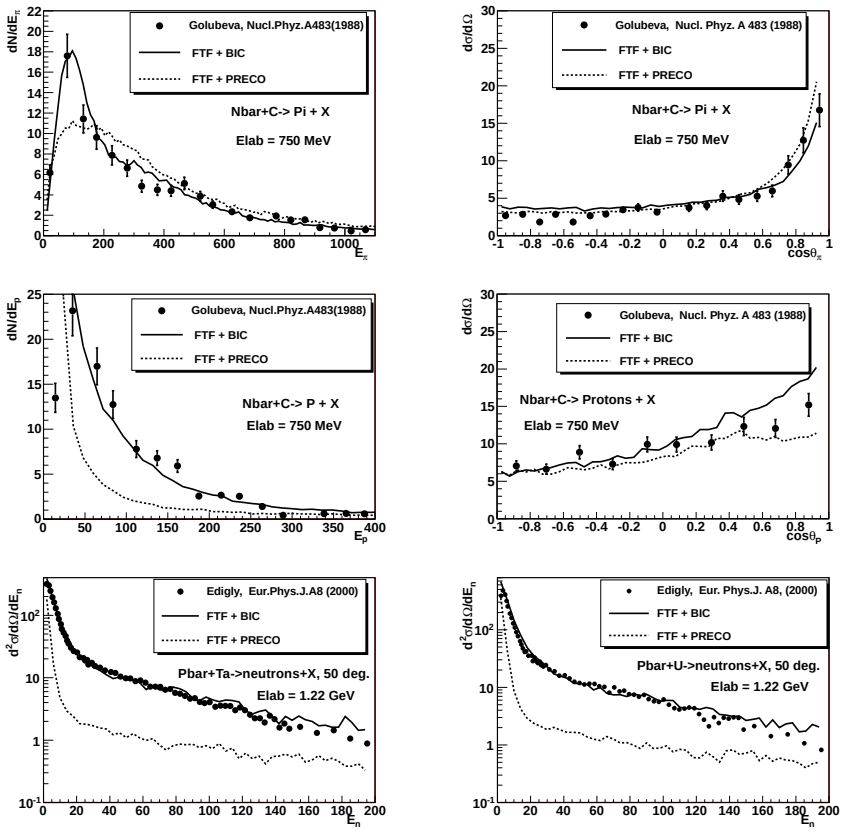

Fig. 4 Inclusive π^+-meson, proton and neutron distributions in $\bar{p}A$- and $\bar{n}A$-interactions. The points are experimental data [21,22], the lines are our calculations.

$$\cdot \left[1 - \frac{1}{A} \int g(\mathbf{b}-\mathbf{s}) \rho_A(\mathbf{s},z) d^2s\, dz\right]^{(\nu_{max}-\nu)A/\nu_{max}},$$

where p_{lab} is a projectile anti-baryon momentum in the target rest frame, and p_0 is a parameter.

Thus at a low energy, only one inelastic interaction of a projectile in a nucleus can happen, but there can be other interactions caused by secondary particles. The secondary particle interactions are mainly responsible for the production of slow neutrons and protons (see Fig. 4). We have checked this using two variants of the model – FTF with the binary cascade model (BIC) and FTF with the precompound de-excitation model (PRECO) [23]. A secondary particle cascading and a nuclear residual de-excitation are considered in the binary cascade model, the second model does not take into account the cascading. Both models BIC and PRECO are presented in the GEANT4 toolkit. As can be seen from a comparison between experimental data [21,22] and model calculations, as depicted in Fig. 4, the finite energy corrections and

the secondary interactions are very important for understanding experimental regularities.

5 Antinucleus-nucleus interactions

To simulate the distribution (8), we use the following algorithm: starting with the expression (7) we ascribe a projectile a power $P = \nu_{max}$. A probability of an interaction with the first nucleon is equal P/ν_{max}. The power decreases after the interaction on unit. The probability of an interaction with the second nucleon is equal to P/ν_{max}, where $P = \nu_{max} - 1$. If the second interaction has happened, the power is decreased one more. In the other case, it is left on the same level. This is applied for each possible interaction. After an annihilation, P is set to zero. The algorithm leads to Eq. (9).

The same algorithm is applied in the case of antinucleus-nucleus interactions using the Glauber inelastic cross sections analogous to Eq. (7). A cascading of secondary particles in the light projectile anti-nuclei is neglected. A result of the calculations is presented in Fig. 5, where the points are experimental data [26], and the line is our calculation.

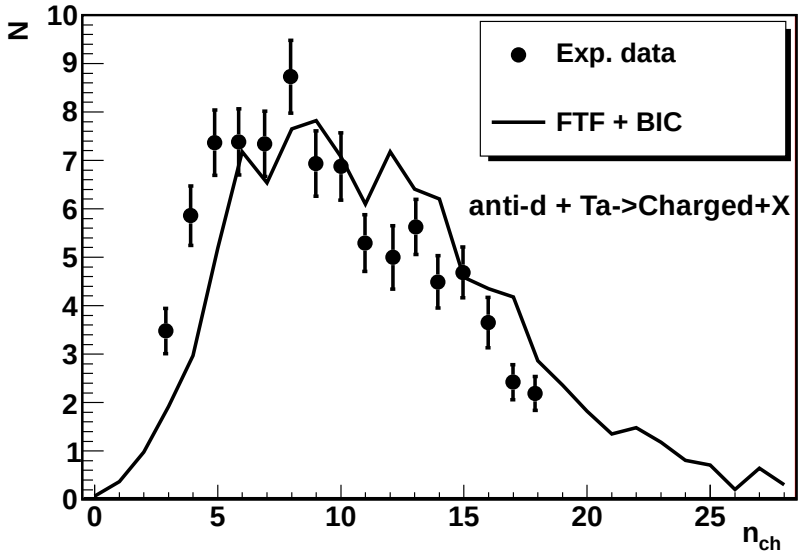

Fig. 5 Charged particle multiplicity distribution in $\bar{d}$ + Ta interactions at a momentum of $P_{\bar{d}} = 6.1$ GeV/c.

There is no other data on light anti-nucleus interactions with heavy materials except [26], though there are a lot of detailed data on $\bar{d}d$- interactions, and only few data on general properties of the interactions.

Conclusion

Using the described approach we have developed in the GEANT4 framework a Monte Carlo model for the simulation of antinucleus-nucleus interactions for the projectiles $\bar{p}, \bar{d}, \bar{t}, {}^3\overline{\mathrm{He}}, {}^4\overline{\mathrm{He}}$. The model is valid between 100 MeV/c and 1 TeV/c per antinucleon. A comparison of the model calculations to available data shows a good agreement sufficient for most applications in cosmic ray experiments and in large HEP experiments including those at the LHC and RHIC.

The GEANT4 toolkit is now able to simulate the antinucleus-nucleus interactions for all target nuclei since version *9.4.p01*.

Acknowledgements The authors are thankful to J. Apostolakis, G. Cosmo, G. Folger, A. Howard, V.N. Ivanchenko and D.H. Wright for stimulating discussions and interest in the work.

References

1. http://pamela.roma2.infn.it/index.php
2. http://www.universe.nasa.gov/astroparticles/programs/bess/
3. http://ams.cern.ch/
4. http://ida1.physik.uni-siegen.de/caprice.html
5. H. Agakishiev et al. (STAR Collaboration), arXiv:1103.3312 [nucl-ex] (2011); B.I. Abelev et al. (STAR Collaboration), Science, **328**, 58 (2010); C. Adler et al. (STAR Collaboration), Phys. Rev. Lett., **87**, 262301 (2001); B.I. Abelev et al. (STAR Collaboration), arxiv: 0909.0566 [nucl-exp] (2009).
6. S. Afanasiev et al. (PHENIX Collaboration), Phys. Rev. Lett., **99**, 052301 (2007); S.S. Adler et al. (PHENIX Collaboration), Phys. Rev. Lett., **94**, 122302 (2005).
7. B. Alver et al. (PHOBOS Collaboration), Phys. Rev., **C77**, 061901(R) (2008).
8. P. Antonioli, arXiv:1010.3735 [hep-ex] (2010).
9. H. Agakishiev et al. (STAR Collaboration), arXiv:1103.3312 (2011).
10. S. Agostinelli (GEANT4 Collaboration), Nucl. Instrum. Methods A, **506**, 250 (2003); J. Allison (GEANT4 Collaboration), IEEE Trans. Nucl. Sci., **53**, 270 (2006).
11. V. Franco, and R.J. Glauber, Phys. Rev., **142**, 142 (1966).
12. O.D. Dalkarov, and V.A. Karmanov, Nucl. Phys., **A445**, 579 (1985).
13. W.W. Buck, J.W. Norbury, L.W. Townsend, and J.W. Wilson, Phys. Rev., **C33**, 234 (1986).
14. Z. Yu-shun, L.Ji-feng, B.A. Robson, and L. Yang-guo, Phys. Rev., **C54**, 332 (1996).
15. B.V. Batyunya et al., JINR preprint **P1-87-523** (1987).
16. V.Franco, Phys. Rev., **175**, 1376 (1968).
17. V. Uzhinsky, J. Apostolakis, A. Galoyan et al., Phys. Lett., **B705**, 235 (2011).
18. S.P. Denisov et al., Nucl. Phys., **B31**, 253 (1971).
19. D.W.L. Sprung and J. Martorell, J. Phys., **A30**, 6525 (1997); J. Phys., **A31**, 8973 (1998).
20. B. Andersson et al., Nucl. Phys., **B281**, 289 (1987); B. Nilsson-Almquist and E. Stenlund, Comp. Phys. Comm., **43**, 387 (1987).
21. Ye.S. Golubeva et al., Nucl Phys., **A483**, 539 (1988).
22. T. von Edigly et al., Eur. Phys. J. **A8**, 197 (2000).
23. http://geant4.web.cern.ch/geant4/UserDocumentation/UsersGuides/PhysicsReferenceManual/fo/PhysicsReferenceManual.pdf
24. Kh. Abdel-Waged and V.V. Uzhinsky, Phys. Atom. Nucl., **60**, 828 (1997); Yad. Fiz., **60**, 925 (1997); Kh. Abdel-Waged and V.V. Uzhinsky, J. Phys., **G24**, 1723 (1997).
25. M.I. Adamovich et al. (EMU-01 Collaboration), Zeit. fur Phys., **A358**, 337 (1997).
26. V.F. Andreyev et al., Nuov. Cim., **103A**, 1163 (1989).